






Research Article

Mechanical Property of Biomodified Geogrid and Reinforced Calcareous Sand

Qiang Ou ¹, Yifu Li ², Yang Yang ¹, Zhaogang Luo ², Shaokang Han ³,
and Tan Zou ⁴

¹College of Civil Engineering, Chongqing University, Chongqing 400045, China

²Key Laboratory of New Technology for Construction of Cities in Mountain Area, Chongqing University, College of Civil Engineering, Chongqing 400045, China

³School of Civil Engineering, Chongqing University, 174 Shazheng Street, Shapingba District, Chongqing, China 400045

⁴Chongqing University Industrial Technology Research Institute, Chongqing, China 400045

Correspondence should be addressed to Yang Yang; yyyong@cqu.edu.cn

Received 28 February 2022; Accepted 12 March 2022; Published 5 April 2022

Academic Editor: Di Feng

Copyright © 2022 Qiang Ou et al. This is an open access article distributed under the Creative Commons Attribution License, which permits unrestricted use, distribution, and reproduction in any medium, provided the original work is properly cited.

The strength and deformation properties of maritime geotechnical structures made primarily of calcareous sand are critical for project safety. The geogrid reinforcement is developed as a promising approach to improve the mechanical properties of calcareous sand. This study investigates the mechanical property of biomodified geogrid via a microbially induced calcite precipitation (MICP) process to improve the effectiveness of geogrid for reinforcement of calcareous sand. A series of unconsolidated undrained triaxial experiments were conducted to evaluate the mechanical property and deformation behaviors of biomodified geogrid and reinforced calcareous sand (BGRCS), taking into consideration the impacts of the geogrid layer, times of biotreatment, and confining pressure. Compared to the untreated geogrid, the strength of the BGRCS is distinctly changed due to the increase roughness, and the deviatoric stress-strain curves are evidently hardening. Strength and pseudocohesive force can be further enhanced by raising the geogrid layer of the reinforced specimens, while internal friction angle also increases the amplitude of variation with the times of biotreatment. The geogrid, times of biotreatment, and confining pressure are all intimately related to the strength and the deformation of the reinforced specimens. The interactions of geogrid ribs and calcareous sand particles are analyzed and friction using scanning electron microscope tests that could provide a reference for revealing the mechanical mechanism of BGRCS.

1. Introduction

Calcareous sands are formed by the remains of marine organisms deposited over a long period of geological action and are characterized by porosity, high calcium carbonate content, and easy fragmentation [1–3]. Between 30°N and 30°S, these widely distributed calcareous sands are a potentially important material source for marine engineering construction. Under a certain stress level, large deformation or even grain breakage could be generated in calcareous sand, posing a major threat to the structural integrity of geotechnical constructions [4–7]. In recent years, large-scale offshore wind turbines [8, 9], subsea energy mining platforms [10,

11], and artificial reefs [12, 13] have all been erected, and their safety must be ensured completely.

Mastering the strength and deformation characteristics of calcareous sand is a basic requirement for the design and safe construction of offshore geotechnical engineering. It is generally believed that the strength and deformation of calcareous sand are affected by particle size gradation, density, and stress state [14–18]. Under the high stress, calcareous sand would undergo obvious particle fragmentation [5]. The fine particles produced by the crushing cause a significant transformation of the mechanical properties. Wei et al. [19] investigated the influence of particle breakage on the shear strength and found that the increase in shear stress was limited due to the intense

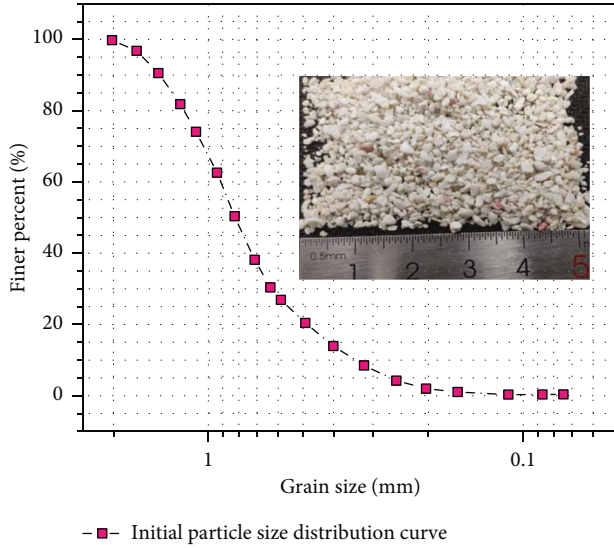


FIGURE 1: Initial grain distribution curve of calcareous sand.

TABLE 1: Physical properties of calcareous sand.

Items	Value
Specific gravity	2.78
Median particle diameter (d_{50}) (mm)	0.82
Uniformity coefficient (C_u)	2.50
Curvature coefficient (C_c)	1.30
Minimum void ratio (e_{\min})	0.79
Maximum void ratio (e_{\max})	1.24

particle breakage and rearrangements. In addition, particle size distribution, particle shape, and particle surface roughness also have significant effects on particle crushing and stress-strain responses [6]. Ground settlement and the associated structural stability can be potentially affected by these fundamental mechanical properties in calcareous sand zone (e.g., the penetration of large diameter piles and the construction of underground pipes) [3, 20–22].

Adopting reinforcement methods, including chemical, biological, and physical methods, can improve the strength and deformation properties of calcareous sands; thus, the safety and stability of geotechnical structures will be significantly improved. For chemical reinforcement [23], chemical substances are difficult to recycle and may pollute the marine environment, causing irreversible environmental damage. Therefore, chemical reinforcement methods are not suitable for large-scale promotion. Physical reinforcement methods usually involve adding some stable materials to the soil, such as common fibers, geotextiles, and geogrids [24–31]. These materials are easy to construct and recycle with obvious effects. Thus geomaterials have the potential for large-scale applications in traditional road foundations, slopes, and retaining walls [29, 32, 33]. Out of the aforementioned geomaterials, geogrids are easy-operated and relatively cheaper. However, their application of geogrids in marine engineering construction is still limited. Recently, an innovative biomodification technique, so-called microbial

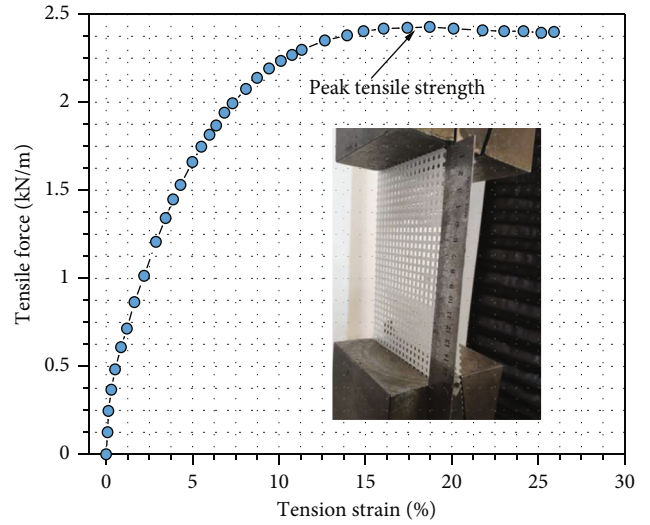


FIGURE 2: The curve of tension-strain for the geogrid.

induced carbonate precipitation (MICP) [15, 34–36], has attracted wide attention on enhancing friction between geomaterials and construction material. For example, Hao et al. 2018 [37] (paper: Enhancing fiber/matrix bonding in polypropylene fiber reinforced cementitious composites by microbially induced calcite precipitation pre-treatment) have studied the improved fiber/matrix bonding of cementitious composites via MICP-modified fiber. Zhang et al. [31] also investigated the effect of MICP-modified steel fiber on the bonding properties of ultrahigh performance concrete.

In this paper, a biomodified small-size geotechnical geogrid via MICP treatment was used to reinforce calcareous sand, enhancing the friction performance of geogrids reinforced calcareous sand. Through a series of unconsolidated undrained triaxial tests (UU), the mechanical and deformation properties of geogrids reinforced calcareous sand with biomodified geogrids and untreated geogrids under different confining pressures were compared. For calcareous sand reinforced by biomodified geogrids, the influence of confining pressures, the layer of the geogrid, and times of biotreatment on the mechanical and deformation performance were also considered. Microscopic interfacial interaction characteristics of biomodified geogrid were analyzed through scanning electron microscope (SEM) tests. The mechanical characteristic of biomodified geogrid reinforcement was also discussed.

2. Materials and Methods

2.1. Materials. The calcareous sand used in the test originated from the South China Sea, which is also typical coral sand [38, 39]. The calcareous sand particles are off-white, irregular in shape, and with a large number of microscopic pores [16, 39]. The dried calcareous sand particles were passed through a 2 mm sieve to remove oversized impurities for triaxial tests. Figure 1 shows the sieved calcareous sand and its particle size distribution curve, and the basic physical property indexes of the calcareous sand are shown in Table 1. Additionally, the specially customized polyethylene geogrid with a small mesh

TABLE 2: Test schemes and initial parameters.

Number	Particle size range (mm)	Geogrid layers	Relative density (%)	Moisture content (%)	Confining pressure (kPa)	Times of biotreatment	Shearing rate (mm·min ⁻¹)
T1	0-2	0	50	0	100/200/300/400	0	0.2
T2	0-2	1	50	0	100/200/300/400	0/1/2/3	0.2
T3	0-2	3	50	0	100/200/300/400	0/1/2/3	0.2
T4	0-2	5	50	0	100/200/300/400	0/1/2/3	0.2

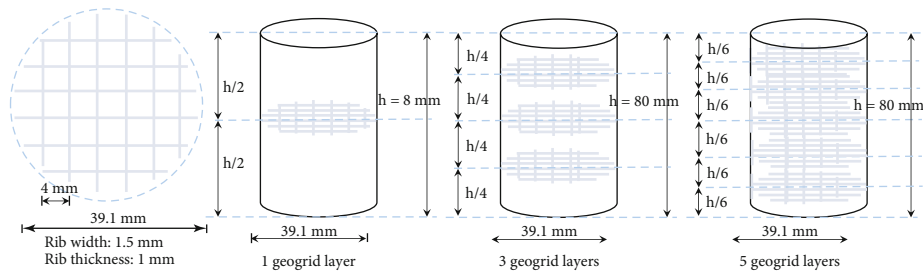


FIGURE 3: Geogrid and layout diagram.

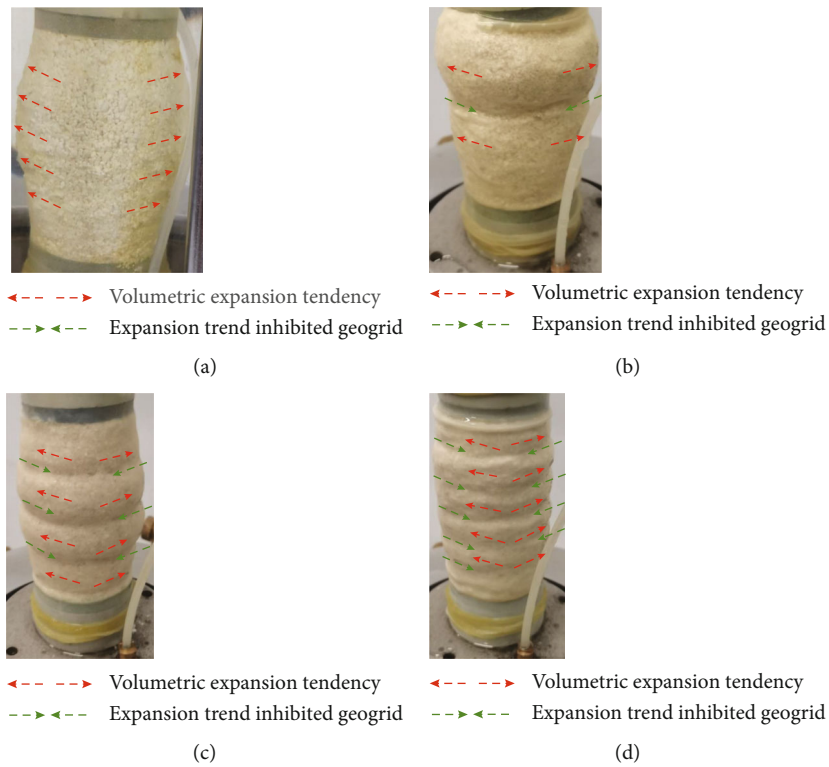
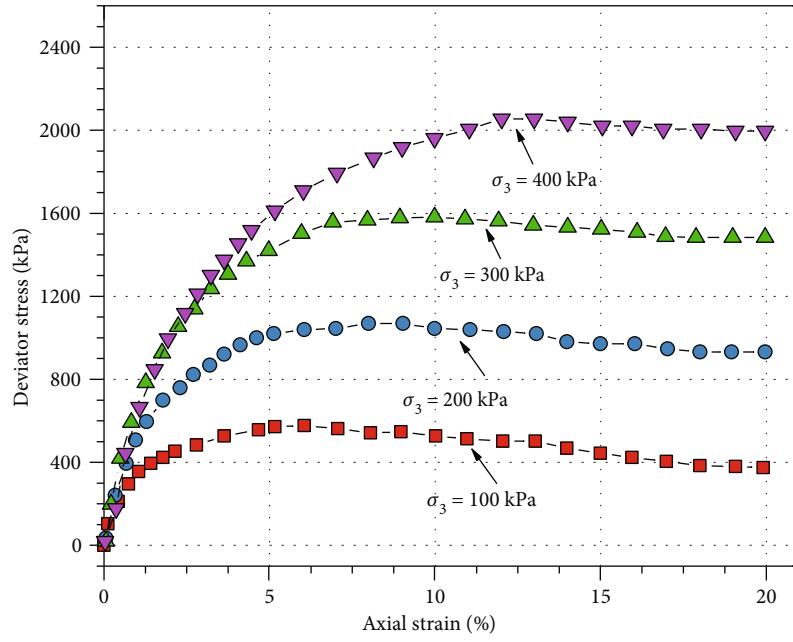
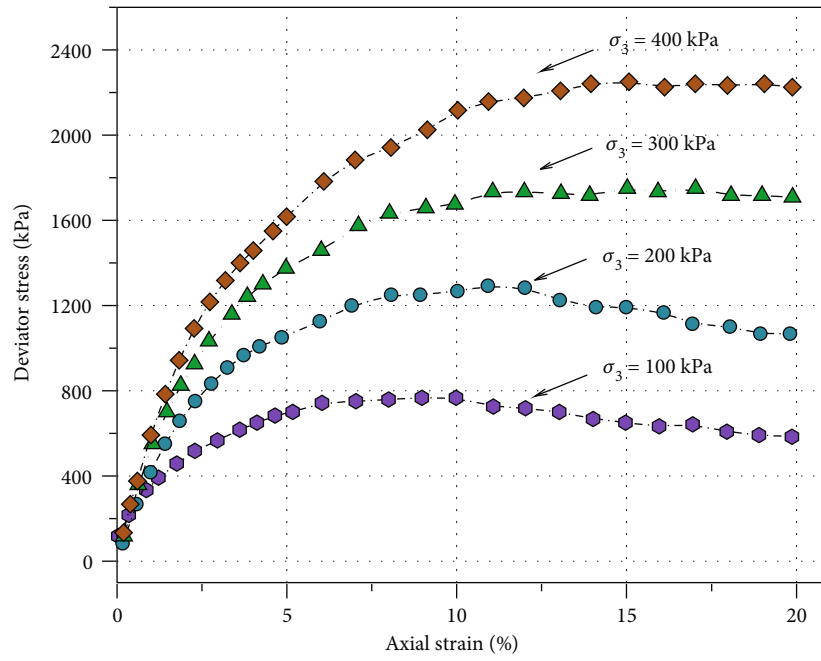


FIGURE 4: Failure modes of specimens at 200 kPa confining pressure: (a) nonreinforced, (b) reinforced by 1 geogrid layer, (c) reinforced by 3 geogrid layers, and (d) reinforced by 5 geogrid layers.



(a)



(b)

FIGURE 5: Continued.

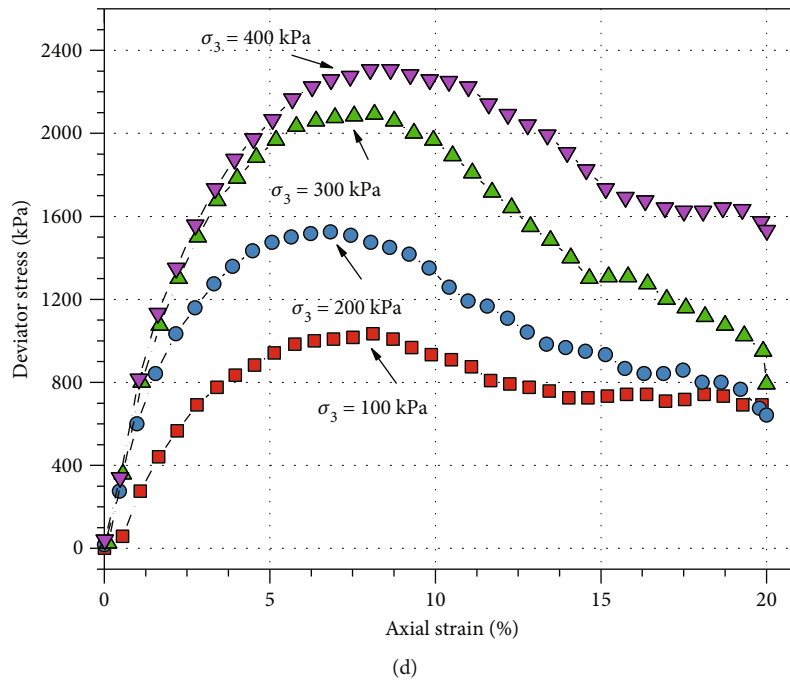
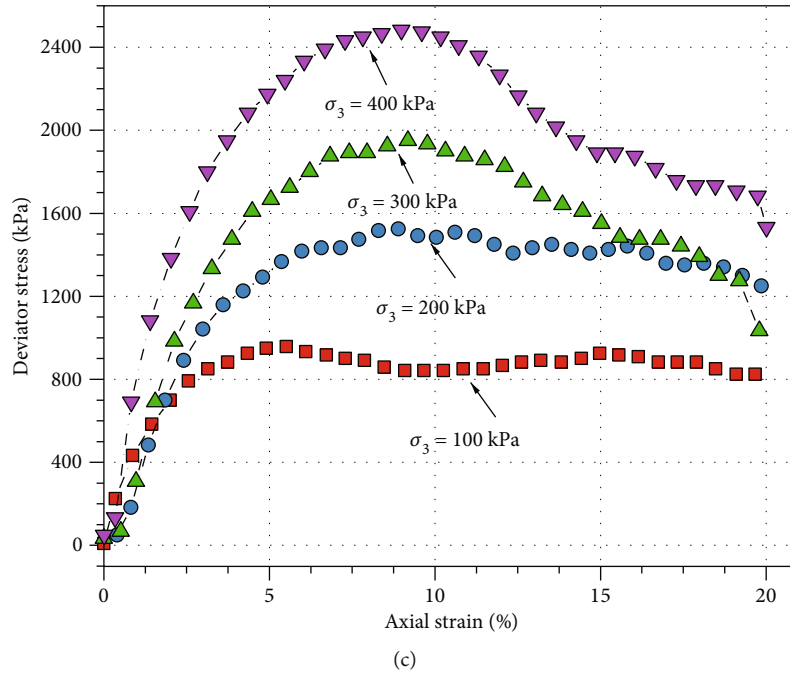


FIGURE 5: Continued.

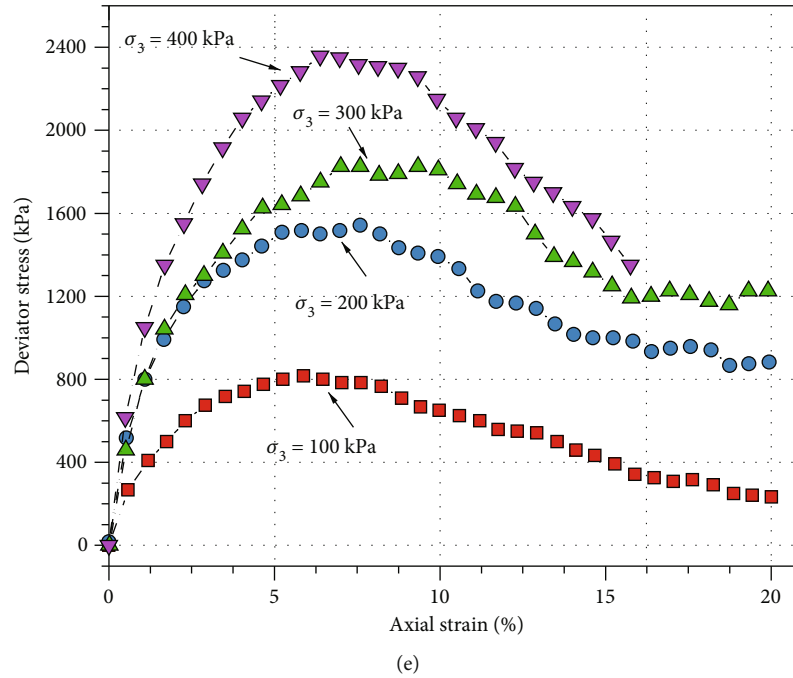


FIGURE 5: Deviatoric stress-strain curves in T1 and T2: (a) 0 time of biotreatment without reinforced layer, (b) 0 time of biotreatment with 1 reinforced layer, (c) 1 time of biotreatment with 1 reinforced layer, (d) 2 times of biotreatment with 1 reinforced layer, and (e) 3 times of biotreatment with 1 reinforced layer.

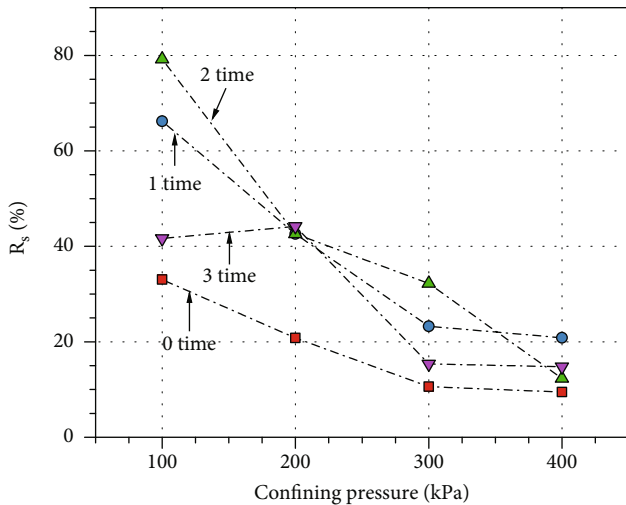


FIGURE 6: The relationship between the peak intensity increasing rate and times of biotreatment in T1 and T2.

size manifests similar properties to the geogrid used in actual engineering projects. Therefore, it can be effectively used for these laboratory tests. The basic tensile performance of the geogrid was obtained from the unidirectional tensile tests in Figure 2, and its ultimate tensile strength exceeds 2.4 kN/m.

2.2. Biomodification Treatment. Commercial *Sporosarcina pasteurii* (DSM33) was used for the biomodification process. The bacteria cultivation process was followed by the same procedure mentioned by Yang et al. [40]. The OD_{600} of the harvested bacterial solution was $2 \sim 2.3$, and the urease activity was $10 \pm$

0.5 U/ml (1 U = 1 mol urea hydrolyzed per minute). The cementation solution used in this study included 1 M of equimolar of urea (60 g/L) and calcium chloride (111 g/L).

Three acrylic tray boxes were used for the MICP treatment of geogrids. The geogrids were soaked into the solution that consisted of bacterial culture (2.5 U/ml diluted by deionized water) and cementation solution with a volume ratio of 1:1. The tray box was kept at room temperature ($25 \pm 2^\circ\text{C}$) for 24 h to allow the calcite generated by the bacteria to be deposited on the surface of geogrids. The volume of biological reagent solution was about 5 times the volume of geogrids. Repeated treatment was carried out every 24 hours by replacing the biological reagent solution. After treatment, geogrids were rinsed with 5 times of tap water and air-dried prior to use. Different times of biotreatment varied from 1 to 3 were conducted to achieve different biomodification by varying the amounts of coating. The calcium carbonate content (CCC) measurement was also conducted using the acid washing method, reported by Choi et al. (2017) [41].

2.3. Triaxial Tests. In order to investigate the basic mechanical properties of biomodified geogrid and reinforced calcareous sand, unconsolidated undrained triaxial tests (UU) were conducted in the laboratory. The effects of geogrid, times of biotreatment, and confining pressure were considered. The specific testing scheme is presented in Table 2. The sample is 39.1 mm in diameter and 80 mm in height. The geogrid was processed into a circular piece with a diameter of slightly less than 39.1 mm, which was divided into 1/3/5 layers of horizontal layout in the sample. Sample sizes and geogrid layout are shown in Figure 3.

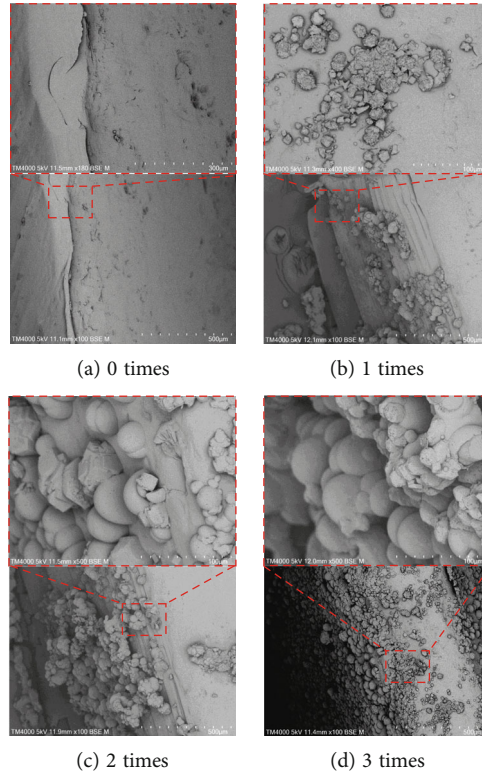


FIGURE 7: SEM of geogrid treated by MICP process.

During the test, the sample was divided into two/four/six parts equally according to the set quality, and the density was strictly controlled. After that, a shear rate of 0.2 mm/min was used for the test. When the axial strain reached 20%, the test was stopped, and the data was sorted out. When the deviated stress-strain curve is softening, the peak strength is taken as the shear strength, whereas the stress corresponding to 15% axial strain is taken as the shear strength when the deviated stress-strain curve is hardening.

3. Results and Analysis

3.1. Failure Patterns. During the test, the loading failure process of each sample was observed, and the typical failure characteristics of some samples were recorded. The test results indicate that the expansion of calcareous sand is quite obvious in the triaxial tests, and most of the samples are bulging during the damage process without any obvious shear surface. Generally, the shearing expansion of calcareous sands is pronounced [19, 39], especially at low confining pressures. Figure 4 compares the failure modes of the unreinforced and the reinforced calcareous sand samples under 200 kPa confining pressure. The lateral bulge of the sample without reinforcement is obvious (Figure 4(a)), and there is no shear surface when it is destroyed. However, the lateral bulge of the reinforced specimens is relatively limited. It can be observed that the reinforced specimens manifest obvious “restraint marks,” limiting the lateral movement of the nearby calcareous sand and thus reducing the deformation. As can be seen, the effect of restraint is more obvious when the layer of geogrid increases. Goodarzi and Shahn-

zari [26] and Rezvani [29] investigated the mechanical properties of geotextile-reinforced calcareous sand and found that the strength could also be significantly increased compared to the unreinforced specimens.

The above results also suggest that increasing the layers of the geogrid reinforcement may be more likely to reduce volumetric expansion tendency leading to significant strength enhancement.

3.2. Deviatoric Stress-Strain Relationship. The strength and deformation characteristics of calcareous sand can be reflected by the stress-strain relationship. The relationships between deviatoric stress and axial strain for reinforced and unreinforced specimens, as well as reinforced specimens with different times of biotreatment, were experimentally compiled, as shown in Figure 5. The deviatoric stress-strain curves of medium-dense calcareous sand ($D_r = 0.5$) show an obvious intensify under the confining pressure at 100 kPa~400 kPa compared the Figures 5(a) and 5(b). The peak stress increased 8.2% compared to the unreinforced sample when the strains corresponded to the peak strengths. Meanwhile, Figures 5(b)–5(e) show the deviatoric stress-strain curves that the sample reinforced by 1 layer of geogrid which treated by different times of biotreatment. With the biomodified geogrid using the MICP process, the deviatoric stress-strain relationships of the calcareous sand specimens in medium-dense states gradually harden, and the strengths are also significantly improved (Figures 5(b)–5(e)). The strength of the geogrid-reinforced calcareous sand was improved with biomodified geogrid, i.e., the strength of the sample with one time biotreatment ($CCC = 0.81\%w/w$)

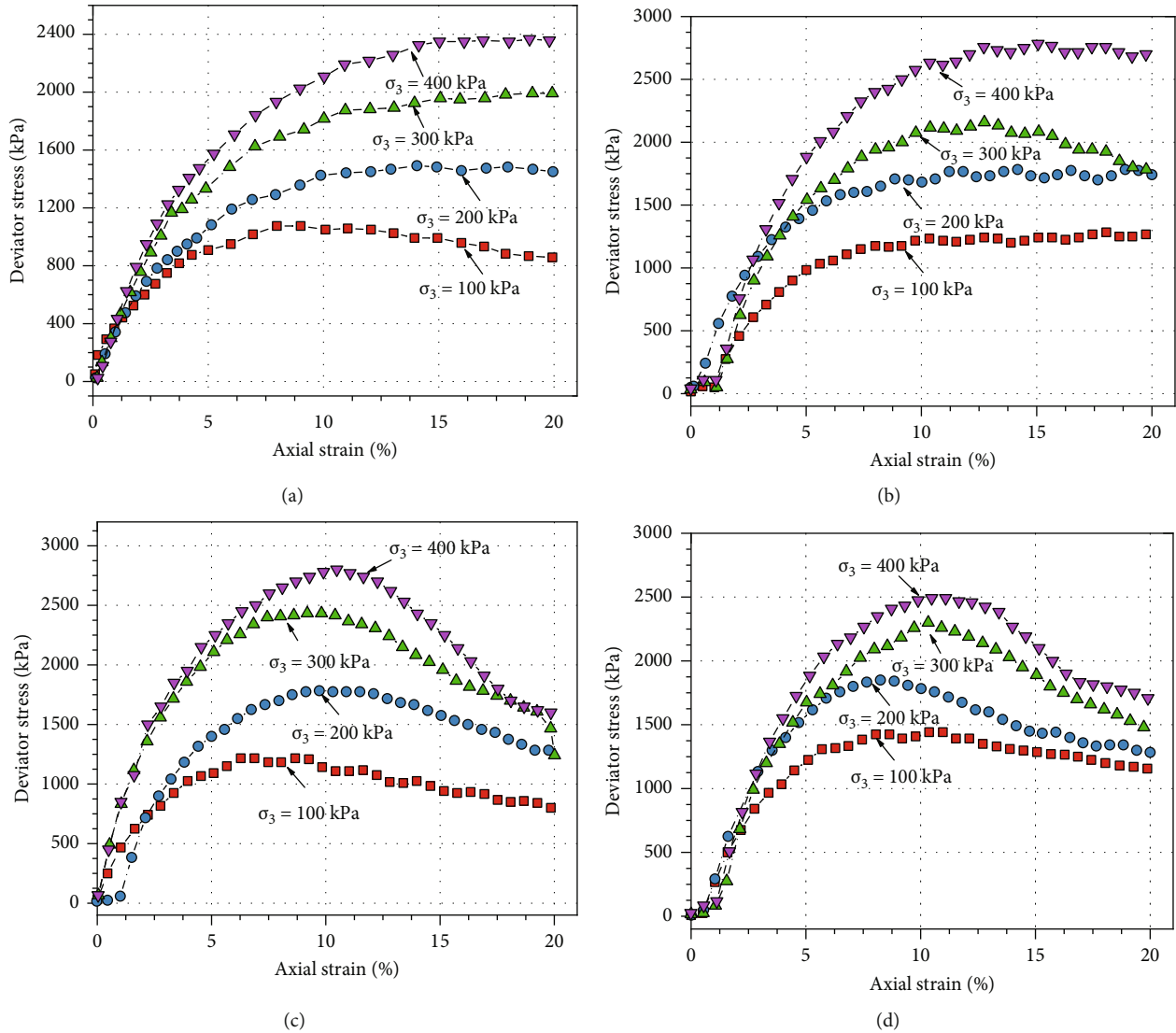


FIGURE 8: Deviatoric stress-strain curves in T3: (a) 0 time of biotreatment with 3 reinforced layers, (b) 1 time of biotreatment with 3 reinforced layers, (c) 2 times of biotreatment with 3 reinforced layers, and (d) 3 times of biotreatment with 3 reinforced layer.

increased 26.4%, 18.0%, 12.5%, and 10.8% when the confining pressure increased from 100 kPa to 400 kPa, respectively. With the two times of biotreatment, the peak intensity of the sample slightly increases. However, the peak intensity decreases when the geogrid was treated 3 times by MICP. More detailed data can be found in Figure 6. It can be seen that the peak intensity increasing rate shows a decreasing trend with the increase of confining pressure. In other words, the biomodified geogrid and its reinforcement effect work relatively well at low confining pressure. This phenomenon can be explained through Figure 7. Figure 7(a) is the SEM of the geogrid without biotreatment, and the surface of untreated geogrid is relatively smooth compared to the geogrid treated by MICP (Figures 7(b)–7(d)). Figures 7(b)–7(d) demonstrate that the geogrids were treated by the MICP at different times, and many CaCO_3 crystals were precipitated on the surface of geogrid. The interface of the biomodified geogrid and calcareous sand becomes rough compared to the sample without biotreatment; thus, the

strength of the triaxial test will significantly increase. A similar observation was observed by Zhang et al. [31]. When the geogrid was treated twice ($\text{CCC} = 1.49\%w/w$), the interface produced more CaCO_3 grain rough in Figure 7(c), and the interface friction was further enhanced. However, the intensity of the sample was further decreased when the geogrid was treated 3 times ($\text{CCC} = 2.13\%w/w$). It can be accounted for the excess CaCO_3 coarse grain affect the interface interaction, which makes the contact interface between geogrid and calcareous sand particles changed into that between CaCO_3 particles and calcareous sand. So, the peak intensity of the sample that was treated 3 times decreased.

These results reveal that using biomodified geogrids to reinforce calcareous sands is an effective way to increase the strength and improve the deformation behavior of GRCS.

Figure 8 shows the stress-strain relationship of the samples reinforced by 3 layers of geogrids which are treated with MICP. Compared with Figure 8(a), the peak intensity of the

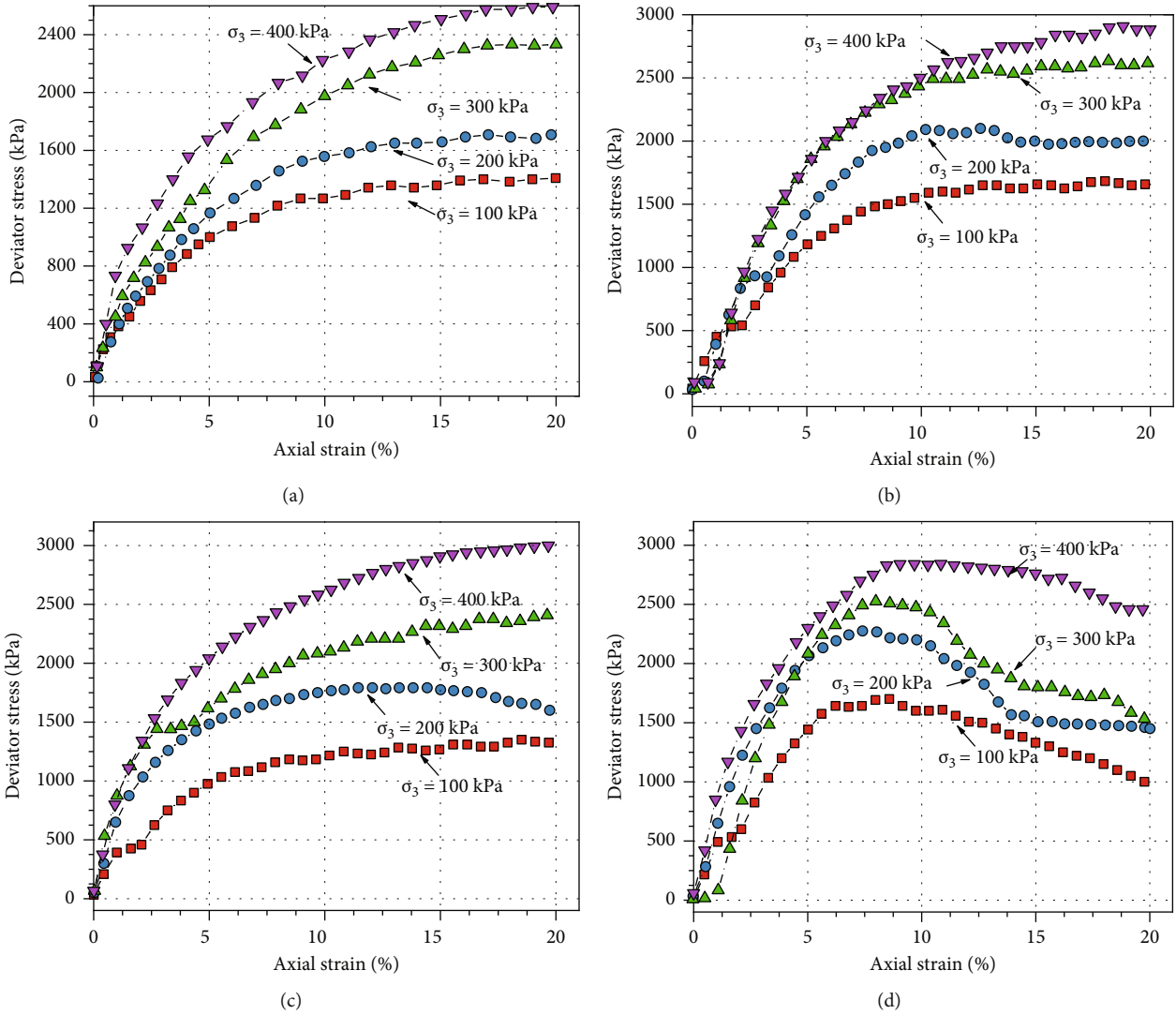


FIGURE 9: Deviatoric stress-strain curves in T4: (a) 0 time of biotreatment, (b) 1 time of biotreatment, (c) 2 times of biotreatment, and (d) 3 times of biotreatment.

samples apparently increases with the introduction of bio-modified geogrids in Figures 8(b)–8(d). Specifically, the peak intensity increased from 1958 kPa to 2158 kPa, about 10.2% when the confining pressure is 300 kPa as shown in Figure 8(b). And the increase rates are 24.3% and 17.4% when the geogrids were treated 2 times and 3 times in Figures 8(c) and 8(d), respectively. It can be concluded that using bio-modified geogrids can enhance the strength of the geogrid reinforced calcareous sand to a certain extent due to the strengthened interface friction by increased roughness. However, the enhancement of the interaction could be diminished when the precipitation is used more than a certain amount. On the other hand, the strength of three layers of geogrids reinforced calcareous sand is generally higher than that of one layer of geogrid reinforced calcareous sand.

Figure 9 shows the stress-strain curves with different times of biotreatment when the calcareous sand was reinforced by 5 layer geogrids. In general, the peak intensity is more than that reinforced by 1 layer geogrid and 3 layer geogrids.

It says that the increase in the number of layers of the geogrid will increase the strength of the sample. Meanwhile, taking the $\sigma_3 = 400$ kPa for example, the peak stress increased from 2592 kPa, to 2908 kPa, 2991 kPa, and 2840 kPa about 12.2%, 15.4%, and 9.6% in Figure 9, respectively. When the geogrids were treated once or twice, the intensity will continue to enhance as the number of treatments increases. However, the effect of the intensity increase will weaken as the geogrids are treated three times.

3.3. Strength Indexes. In order to evaluate the strength enhancement effect of the BGRCS, the strength of the T1 specimens is used as a benchmark to calculate the strength enhancement rate of the remaining specimens, R_s . The R_s is defined as follows.

$$R_s = \frac{\sigma_{if} - \sigma_{of}}{\sigma_{of}} \times \%, \quad (1)$$

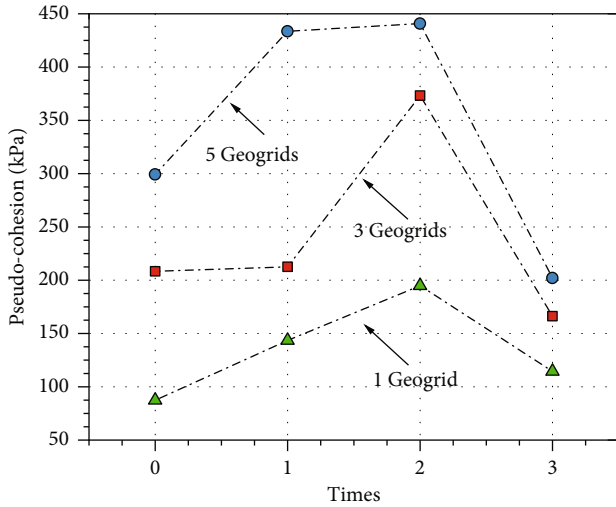


FIGURE 10: The pseudocohesive force with different times of biotreatment.

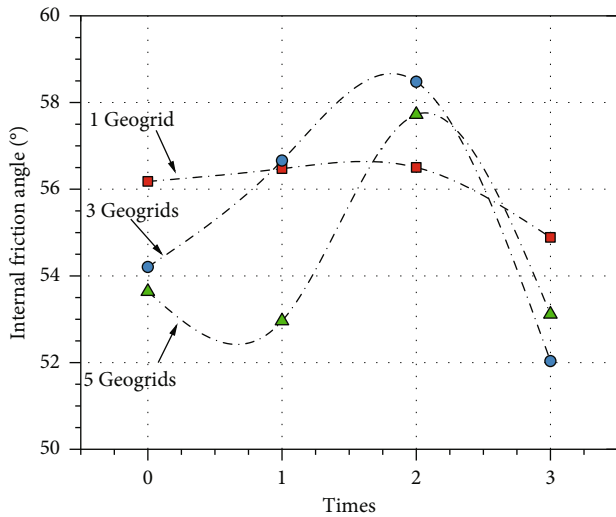


FIGURE 11: Variation of internal friction angle with the layer of biomodified geogrid.

where the σ_{of} is the shear strength of the T1 specimen under a specific confining pressure, and the σ_{if} is the shear strength of a biomodified geogrid and reinforced specimen under the corresponding confining pressure. The strength enhancement rates of all BGRCS are presented in Figure 6. The R_s tends to be lower with the increasing confining pressure, implying that the reinforcing effect of the geogrids is more obvious at lower confining pressure. For the four groups of reinforced specimens with different times of biotreatment, the R_s also increases with the increasing number of treatments when the treatments are less than twice. After that, the R_s trends to be a lower state. The reason can be the same as the above sections.

The cohesion of calcareous sand is generally considered to be zero. Natural sandy soils also manifest a certain pseudocohesive force [42–44] related to the intergranular occlusion and suction in the case of unsaturated sands [45, 46]. When geogrids

are used to reinforce calcareous sands, the mesh of the geogrids generates a restraining effect, which results in a significant pseudocohesion. In addition, biotreatment can further improve the intensity of the reinforced calcareous sands. As shown in Figure 10, the pseudocoheions are calculated by compiling the experimental data for different times of biotreatment and the layer of the geogrids. The results show that the pseudocohesion is significantly affected by the layer of the geogrids, and it increases with increasing the layer of the geogrid. At the same time, the pseudocohesion is significantly affected by the times of biotreatment, and the pseudocohesion gradually increases when the biotreatment times are less than 2, while the pseudocohesion would decrease when the geogrids were treated 3 times.

Figure 11 displays the variation of internal friction angle with the layer of biomodified geogrids. It can be seen from Figure 11 that the change range is wider when the geogrid is more than 1 layer. The results show that the internal friction angle will firstly increase and then decrease with increasing times that the geogrid was treated. The internal friction angle follows a common similar pattern with the pseudocohesion. The results discussed above indicated that the coarse particles reinforced by the biomodified geogrids would form a larger pseudocohesion and a little change for internal friction angle.

4. Conclusions

This study focuses on the strength and deformation properties of the biomodified geogrid and reinforced calcareous sand (BGRCS). Through a series of unconsolidated undrained triaxial tests and scanning electron microscope tests, the effects of the layer of the geogrid, times of biotreatment, and confining pressure on the stress-strain response, strength indexes, and failure patterns of biomodified and reinforced calcareous sand were investigated. Combining the presented experimental results and microscopic interface analysis, the mechanical property of BGRCS has been discussed. The following conclusions can be obtained:

- (1) From the failure patterns of the reinforced samples, increasing the layers of the geogrid reinforcement can reduce volumetric expansion tendency, consequently leading to significant strength enhancement
- (2) In comparison with the unreinforced calcareous sand specimens, the strength of the reinforced specimens can be significantly enhanced by about 33.0%, 86.4%, and 135.5% for 1 layer geogrid, 3 layer geogrids, and 5 layer geogrids in this test. The overall strength is improved with increasing the layer of the geogrids
- (3) The strength of the biomodified and reinforced specimens can be significantly improved by about 24.9%, 34.7%, and 6.5% after 1 time, 2 times, and 3 times of biotreatment. As such, reasonable use of biomodified geogrids can improve the strength of geogrid reinforced calcareous sand by increasing the roughness of geogrids so as to the interface

friction properties, but the excessive coating resulted from additional biotreatment could reduce the strength of the geogrids reinforced calcareous sand

- (4) The strength enhancement rate in geogrid reinforced specimens is relatively large at low confining pressure and tends to decrease with the increasing confining pressure. The pseudocohe-sion also improved by the MICP process, reaching a maximum value when the samples were treated twice, then slightly decreasing with additional biotreatment

Data Availability

The datasets and materials used and/or analyzed during the current study are available from the corresponding author on reasonable request.

Conflicts of Interest

The authors declare that they have no conflicts of interest.

Authors' Contributions

Qiang Ou administered the project, provided resources, conceptualized and supervised the study, and reviewed and edited the article. Yi-fu Li investigated the study, contributed to data curation, performed formal analysis, and wrote the original draft. Yang Yang conceptualized and supervised the study, contributed to data curation, performed formal analysis, and wrote the original draft. Zhao-gang Luo investigated and supervised the study and wrote the original draft. Shao-kang Han investigated the study and supervised the study and wrote the original draft. Tan Zou investigated the study and reviewed and edited the article.

Acknowledgments

This work was supported by the National Natural Science Foundation of China (No. 52108299 and No. 52108300) and the China Postdoctoral Science Foundation (No. 2021M693740).

References

- [1] G. R. McDowell and M. D. Bolton, "Effect of particle size distribution on pile tip resistance in calcareous sand in the geotechnical centrifuge," *Granular Matter*, vol. 2, no. 4, pp. 179–187, 2000.
- [2] H. Shahnazari and R. Rezvani, "Effective parameters for the particle breakage of calcareous sands: an experimental study," *Engineering Geology*, vol. 159, pp. 98–105, 2013.
- [3] X.-Z. Wang, Y.-Y. Jiao, R. Wang, M.-J. Hu, Q.-S. Meng, and F.-Y. Tan, "Engineering characteristics of the calcareous sand in Nansha Islands, South China Sea," *Engineering Geology*, vol. 120, no. 1–4, pp. 40–47, 2011.
- [4] Y. Lv, J. Liu, and Z. Xiong, "One-dimensional dynamic compressive behavior of dry calcareous sand at high strain rates," *Journal of Rock Mechanics and Geotechnical Engineering*, vol. 11, no. 1, pp. 192–201, 2019.
- [5] Y. R. Lv, X. Li, and Y. Wang, "Particle breakage of calcareous sand at high strain rates," *Powder Technology*, vol. 366, pp. 776–787, 2020.
- [6] R. Rezvani, A. Nabizadeh, and M. Amin Tutunchian, "The effect of particle size distribution on shearing response and particle breakage of two different calcareous soils," *The European Physical Journal Plus*, vol. 136, no. 10, 2021.
- [7] B. Yuan, Z. Li, Z. Zhao, H. Ni, Z. Su, and Z. Li, "Experimental study of displacement field of layered soils surrounding laterally loaded pile based on transparent soil," *Journal of Soils and Sediments*, vol. 21, no. 9, pp. 3072–3083, 2021.
- [8] K. Trojnar, "Multi scale studies of the new hybrid foundations for offshore wind turbines," *Ocean Engineering*, vol. 192, p. 106506, 2019.
- [9] X. Yang, X. W. Zeng, and X. F. Wang, "Lateral-moment loading capacity and bearing behavior of suction bucket foundations for offshore wind turbines in sand," *International Journal of Geomechanics*, vol. 18, no. 11, article 04018152, 2018.
- [10] E. Dallavalle, M. Cipolletta, V. C. Moreno, V. Cozzani, and B. Zanuttigh, "Towards green transition of touristic islands through hybrid renewable energy systems. A case study in Tenerife, Canary Islands," *Renewable Energy*, vol. 174, pp. 426–443, 2021.
- [11] D. Depellegrin, C. Venier, Z. Kyriazi et al., "Exploring multi-use potentials in the Euro-Mediterranean sea space," *Science of the Total Environment*, vol. 653, pp. 612–629, 2019.
- [12] D. Kim, S. Jung, and W. B. Na, "Evaluation of turbulence models for estimating the wake region of artificial reefs using particle image velocimetry and computational fluid dynamics," *Ocean Engineering*, vol. 223, p. 108673, 2021.
- [13] O. Ly, A. I. Yoris-Nobile, N. Sebaibi et al., "Optimisation of 3D printed concrete for artificial reefs: biofouling and mechanical analysis," *Construction and Building Materials*, vol. 272, article 121649, 2021.
- [14] H. X. Huang, Y. M. Chen, J. P. Wang, H. L. Liu, X. Z. Zhou, and Z. G. Huo, "Ring shear tests on shear strength of calcareous sand," *Rock and Soil Mechanics*, vol. 39, no. 6, pp. 2082–2088, 2018.
- [15] L. Liu, H. L. Liu, A. W. Stuedlein, T. M. Evans, and Y. Xiao, "Strength, stiffness, and microstructure characteristics of bio-cemented calcareous sand," *Canadian Geotechnical Journal*, vol. 56, no. 10, pp. 1502–1513, 2019.
- [16] Y. R. Lv, X. Li, C. F. Fan, and Y. C. Su, "Effects of internal pores on the mechanical properties of marine calcareous sand particles," *Acta Geotechnica*, vol. 16, no. 10, pp. 3209–3228, 2021.
- [17] J. Q. Shi, W. Haegeman, and V. Cnudde, "Anisotropic small-strain stiffness of calcareous sand affected by sample preparation, particle characteristic and gradation," *Geotechnique*, vol. 71, no. 4, pp. 305–319, 2021.
- [18] Y. P. Yin, L. Wang, W. Zhang, Z. Zhang, and Z. Dai, "Research on the collapse process of a thick-layer dangerous rock on the reservoir bank," *Bulletin of Engineering Geology and the Environment*, vol. 81, no. 3, pp. 1–11, 2022.
- [19] H. Z. Wei, X. X. Li, S. D. Zhang, T. Zhao, M. Yin, and Q. S. Meng, "Influence of particle breakage on drained shear strength of calcareous sands," *International Journal of Geomechanics*, vol. 21, no. 7, 2021.
- [20] Y. H. Tian and M. J. Cassidy, "Pipe-soil interaction model incorporating large lateral displacements in calcareous sand," *Journal of Geotechnical and Geoenvironmental Engineering*, vol. 137, no. 3, pp. 279–287, 2011.

- [21] B. Yuan, Z. Li, Z. Su, Q. Luo, M. Chen, and Z. Zhao, "Sensitivity of multistage fill slope based on finite element model," *Advances in Civil Engineering*, vol. 2021, Article ID 6622936, 13 pages, 2021.
- [22] J. G. Zhang, D. P. Stewart, and M. F. Randolph, "Modeling of shallowly embedded offshore pipelines in calcareous sand," *Journal of Geotechnical and Geoenvironmental Engineering*, vol. 128, no. 5, pp. 363–371, 2002.
- [23] B. Yuan, Z. Li, Y. Chen et al., "Mechanical and microstructural properties of recycling granite residual soil reinforced with glass fiber and liquid-modified polyvinyl alcohol polymer," *Chemosphere*, vol. 286, article 131652, Part 1, 2022.
- [24] N. C. Consoli, M. D. T. Casagrande, A. Thome, F. D. Rosa, and M. Fahey, "Effect of relative density on plate loading tests on fibre-reinforced sand," *Geotechnique*, vol. 59, no. 5, pp. 471–476, 2009.
- [25] A. P. S. Dos Santos, N. C. Consoli, and B. A. Baudet, "The mechanics of fibre-reinforced sand," *Geotechnique*, vol. 60, no. 10, pp. 791–799, 2010.
- [26] S. Goodarzi and H. Shahnazari, "Strength enhancement of geotextile-reinforced carbonate sand," *Geotextiles and Geomembranes*, vol. 47, no. 2, pp. 128–139, 2019.
- [27] P. Guo, X. Gong, Y. Wang, H. Lin, and Y. Zhao, "Minimum cover depth estimation for underwater shield tunnels," *Tunnelling and Underground Space Technology*, vol. 115, article 104027, 2021.
- [28] I. N. Markou, "A study on geotextile-sand Interface behavior based on direct shear and Triaxial compression tests," *International Journal of Geosynthetics and Ground*, vol. 4, no. 1, 2018.
- [29] R. Rezvani, "Shearing response of geotextile-reinforced calcareous soils using monotonic triaxial tests," *Marine Georesources & Geotechnology*, vol. 38, no. 2, pp. 238–249, 2020.
- [30] M. Shamsi, A. Ghanbari, and J. Nazariafshar, "Behavior of sand columns reinforced by vertical geotextile encasement and horizontal geotextile layers," *The Geomechanics and Engineering*, vol. 19, no. 4, pp. 329–342, 2019.
- [31] D. Zhang, M. A. Shahin, Y. Yang, H. Liu, and L. Cheng, "Effect of microbially induced calcite precipitation treatment on the bonding properties of steel fiber in ultra-high performance concrete," *Engineering*, vol. 50, article 104132, 2022.
- [32] A. Munawir, "Bearing capacity improvement of shallow foundation on multilayered geogrid reinforced sand," *International Journal of Geomate*, vol. 18, no. 69, pp. 216–223, 2020.
- [33] H. Wei, T. Zhao, Q. Meng, X. Wang, and J. He, "Experimental evaluation of the shear behavior of fiber-reinforced calcareous sands," *International Journal of Geomechanics*, vol. 18, no. 12, p. 04018175, 2018.
- [34] M. J. Cui, J. J. Zheng, J. Chu, C. C. Wu, and H. J. Lai, "Bio-mediated calcium carbonate precipitation and its effect on the shear behaviour of calcareous sand," *Acta Geotechnica*, vol. 16, no. 5, pp. 1377–1389, 2021.
- [35] Y. J. Li, Z. Guo, L. Z. Wang, Z. Ye, C. F. Shen, and W. J. Zhou, "Interface shear behavior between MICP-treated calcareous sand and steel," *Journal of Materials in Civil Engineering*, vol. 33, no. 2, article 04020455, 2021.
- [36] P. Xiao, H. L. Liu, A. W. Stuedlein, T. M. Evans, and Y. Xiao, "Effect of relative density and biocementation on cyclic response of calcareous sand," *Canadian Geotechnical Journal*, vol. 56, no. 12, pp. 1849–1862, 2019.
- [37] Y. Hao, L. Cheng, H. Hao, and M. A. Shahin, "Enhancing fiber/matrix bonding in polypropylene fiber reinforced cementitious composites by microbially induced calcite precipitation pretreatment," *Cement and Concrete Composites*, vol. 88, pp. 1–7, 2018.
- [38] X. M. Ding, W. T. Deng, Y. Peng, H. Zhou, and C. Y. Wang, "Bearing behavior of cast-in-place expansive concrete pile in coral sand under vertical loading," *China Ocean Engineering*, vol. 35, no. 3, pp. 352–360, 2021.
- [39] Y. Wu, N. Li, X. Wang et al., "Experimental investigation on mechanical behavior and particle crushing of calcareous sand retrieved from South China Sea," *Engineering Geology*, vol. 280, p. 105932, 2021.
- [40] Y. Yang, J. Chu, H. Liu, and L. Cheng, "Construction of water pond using bioslurry-induced biocementation," *Journal of Materials in Civil Engineering*, vol. 34, no. 3, p. 06021009, 2022.
- [41] S. G. Choi, S. S. Park, S. Wu, and J. Chu, "Methods for calcium carbonate content measurement of biocemented soils," *Journal of Materials in Civil Engineering*, vol. 29, no. 11, p. 06017015, 2017.
- [42] D. H. Gray and T. Alrefeai, "Behavior of fabric-versus fiber-reinforced sand," *Journal of the Geotechnical Engineering*, vol. 112, no. 8, pp. 804–820, 1986.
- [43] F. Schlosser and N. T. Long, "Recent results of French research on reinforced earth," *Journal of the Construction Division*, vol. 100, no. 3, pp. 223–237, 1974.
- [44] C. S. Wu and Y. S. Hong, "Laboratory tests on geosynthetic-encapsulated sand columns," *Geotextiles and Geomembranes*, vol. 27, no. 2, pp. 107–120, 2009.
- [45] W. J. Likos, A. Wayllace, J. Godt, and N. Lu, "Modified direct shear apparatus for unsaturated sands at low suction and stress," *Geotechnical Testing Journal*, vol. 33, no. 4, pp. 286–298, 2010.
- [46] Y. Tang, T. Vo, H. A. Taiebat, and A. R. Russell, "Influences of suction on plate load tests on unsaturated Silty Sands," *Journal of Geotechnical and Geoenvironmental Engineering*, vol. 144, no. 8, p. 04018043, 2018.